# Lawrence Berkeley National Laboratory
**Recent Work**

**Title**
X-RAY PHOTOEMISSION SPECTRA OF THE VALENCE BANDS OF THE 3d TRANSITION METALS, Sc TO Fe

**Permalink**
https://escholarship.org/uc/item/1j02g91h

**Author**
Ley, L.

**Publication Date**
1977-03-01

U U U U 4 7 I U 4 U U

# X-RAY PHOTOEMISSION SPECTRA OF THE VALENCE BANDS OF THE 3d TRANSITION METALS, Sc TO Fe

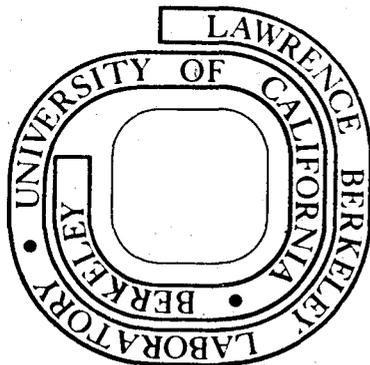L. Ley, O. B. Dabbousi, S. P. Kowalczyk,
F. R. McFeely, and D. A. Shirley

March 1977

## DISCLAIMER

X-RAY PHOTOEMISSION SPECTRA OF THE VALENCE BANDS
OF THE 3d TRANSITION METALS, Sc to Fe [*]

L. Ley,[†] O. B. Dabbousi,[‡] S. P. Kowalczyk,[†]
F. R. McFeely,[‡] and D. A. Shirley

Materials and Molecular Research Division
Lawrence Berkeley Laboratory
and
Department of Chemistry
University of California
Berkeley, California 94720

March 1977

## ABSTRACT

High resolution XPS-valence band (VB) spectra are presented of

the 3d transition metals, Sc to Fe. The measurements were conducted

under ultrahigh vacuum conditions using polycrystalline samples. In

the hcp elements Sc and Ti the main peaks in the valence bands are

identified and compared with the results of band structure calculations.

Some rigidity is observed in the Sc and Ti bands as well as in the

V and Cr bands. The expected two-peak structure for V and Cr is

observed. In chromium we also observed a relatively low density of

states at the Fermi energy ($E_F$). The VB spectrum for chromium is

compared to theoretical predictions, and we present an assignment

of the Cr symmetry point energies. Our valence-band spectrum of Mn

is quite similar to that of Hüfner and Wertheim and our spectrum of Fe is

in good agreement with that observed by Höchst, Goldman, and Hüfner.

These iron VB spectra agree with expectations based on band models

of ferromagnetism. It is observed that the VB spectrum of bcc iron

may be constructed from two bcc Cr VB's shifted to account for spin polarization.  We also deduce the symmetry point energies in iron.

## I.   INTRODUCTION

The 3d transition elements comprise an interesting group of metals, exhibiting a wide variety of structural and electromagnetic properties.  A key factor in the understanding of these metals is the peculiar nature of their electronic band structures.  The valence bands may be considered to arise from the nearly degenerate 3d and 4s atomic levels.  These levels have very different spatial distributions, with the 4s electrons extending considerably beyond the average radius of the 3d shell.  Thus the valence bands of the 3d metals are of two distinct types, a wide band of predominately 4s character resembling the valence bands of simple metals, and a set of narrow, more correlated d-like bands.  The s-like electrons are believed to be the primary source of bonding in the metals,[1] while the narrow atomic-like d-bands give rise to such phenomena as ferromagnetism[2].

Detailed and quantitative knowledge of the valence-band (VB) density of states (DOS), $N(E)$, is rather essential since many theories of the magnetic properties of the transition metals take d-band width, total band width and the DOS at the Fermi level as essential one-electron properties responsible for magnetic behavior.  Electronic specific heat data, conductivity measurements, and the de Haas-van Alphen effect, to mention only a few, sample the electronic properties only within $\sim kT$ of the Fermi energy; thus information on the more tightly-bound states is necessarily indirect.  Spectroscopic methods such as soft x-ray emission spectroscopy (SXS),[3-7] ultraviolet

and x-ray photoemission (UPS, XPS)[8-15] and optical reflectivity measure-
ments are free of these limitations and have contributed valuable
information about the overall features of N(E) for most of the metals
under consideration here.

A straightforward interpretation of SXS and low-energy ($h\nu$ < 40 eV)
UPS data in terms of only the initial density of states is rather
difficult in most cases.  In SXS, the initial-state core vacancy may
distort the valence-band density of states severely.  Examples of such
distortions are well documented in the emission spectra of the alkali
metals.[16]  Low-energy UV photoemission spectra are commonly interpreted
in one of two ways; the direct transition model,[17] in which $\vec{k}$-conser-
vation is an important selection rule and the non-direct-transition
model.[18]  In either case the measured spectrum will contain features
reflecting both the initial electron state and the final electron
state subject to the restriction of energy conservation.  Starting
with a reliable band-structure calculation, an interpretation of the
UPS spectrum in terms of initial- and final-state properties is possi-
ble, and it can yield very detailed results.[19-21]

XPS measurments, however, are free from such limitations, for
with increasing excitation energy $h\nu$, the $\vec{k}$ selection rule is readily
fulfilled without introducing additional structure.  This is expected
from the high and uniform density of available states over the whole
range of $\vec{k}$-space at energies large compared to the energy variations
of the lattice potential.  Experimental evidence for this fact is
well documented[22] and the interpretation of high energy spectra in
terms of initial state density has been highly successful.[23]

In this report our objective is to present a systematic study

of the density of states of the first-row transition metals Sc through

Fe. In an unpublished earlier report,[24] results concerning these

elements were presented. In that report, the position of the Fermi

level for some of these metals were in error. The Fermi levels for

these metals has been redetermined and some of the spectra have been

repeated. This report, therefore, should supercede our previously

reported data. Experimental details are given in Section II and

results are presented in Section III. Of the elements reported here,

Fe[15,25-28] and Mn[27] have been studied earlier by XPS methods. We

shall refer to these works and present a discussion of our results

in Section IV.

## II. EXPERIMENTAL

All the specimens were studied in a Hewlett-Packard 5950A elec-

tron spectrometer with a monochromatized Al Kα (1486.6 eV) x-ray

source. The instrumental resolution is 0.55(2) eV as previously

measured from the broadening of the sharp Fermi edge of a number of

metals.[29]

The spectrometer has been modified for ultra-high vacuum opera-

tion, and was baked out at 200°C before the start of this series of

experiments, obtaining a base pressure of $\leq 2 \times 10^{-10}$ Torr. All the

samples were prepared in situ. Films of Ti, V, Cr, Mn, and Fe were

prepared by d.c. sputtering from high-purity single crystals onto

stainless steel substrates in an ultra-pure argon atmosphere. Sc,

Ti, and V specimens were prepared by vapor deposition onto stainless

steel substrates. Ta or W filaments were used and the evaporation
charges were either single crystals or ultra-pure (better than 99.99%)
polycrystalline material. Before evaporation, the filament and
charge were vigorously outgassed. In most cases, the vacuum during
evaporation was $1 \times 10^{-9}$ Torr or better, and the worst case was $5 \times 10^{-9}$
Torr. A bulk sample, cleaned with a mechanical scraper, was also
used in the Cr case. The different methods of sample preparation
gave identical valence band spectra. Each sample was checked for
impurities such as imbedded argon, surface contaminants (oxygen and
carbon), and possible evaporated filament material (W, Ta) immediately
after preparation, by scanning the region from 0 - 1280 eV binding
energy. In addition to the wide scans, 20 eV scans of the O 1s and
C 1s regions were monitored. The only contamination observed in
these experiments was oxygen. The spectra reported here are from
specimens on which no oxygen signal could be observed initially.
Some of the metals showed oxygen build-up in the course of the measure-
ments; however, no photoemission lines were detected from the forma-
tion of an oxide, even from samples with the largest oxygen 1s signals.
Whenever the oxygen signal reached a level of ∿0.5 monolayer coverage,
a new sample was prepared.[30,31] The average time for the measurement
of a valence band spectrum was about 8 hours, while scandium speci-
mens could be kept in the spectrometer vacuum for over 24 hours with
no detectable oxygen build up; the chromium samples had to be
recleaned after about one hour of running. The number of counts per
channel on the valence band spectra reflects the length of time the

sample could be studied.  For the chromium runs, the Cr $^2P_{3/2}$ and the

O 1s lines were scanned before and after each run.  This enabled

us to use the relative photoionization cross-sections reported by

Leckey[32] to ascertain the oxygen contamination.  The ratios of the

peak heights of the Cr $^2P_{3/2}$ to the O 1s peak was greater than 20

after each of the runs that are incorporated in the final spectrum.

These individual runs, although suffering from poor statistics,

seemed to give undistorted valence-band spectra and when added gave

a spectrum identical to the one reported here.

## III.  RESULTS

The XPS spectra I(E), of the valence-band regions of the transi-

tion metals reported here, Sc through Fe, are shown in Figs. 1 and 2.

In these spectra each point represents the sum of the counts in four

adjacent channels.  The solid curves are straight-line segments, join-

ing the experimental points.  Structural features (i.e., characteristic

peaks, shoulders and edges) of the XPS valence band spectra I(E) of

each element are denoted by letters in Figs. 1 and 2 and the energies

(referred to the Fermi level $E_F$) are given in Table I.  Sharp decreases

in intensity at the Fermi level in Sc, Co, Ni, and Au define $E_F$ to

better than ±0.05 eV in a single determination.  However, instrumental

drift over the course of these runs necessitated repeated determina-

tion of the Fermi level.  We used the above standards, cross-checked

the reported Fermi levels of the samples and used our known instru-

mental resolution as a check of our determination of the Fermi levels.

The uncertainty in the reported Fermi level is ∿±0.05 eV for all

samples except Cr where the uncertainty in the value of the Fermi

level is ∿±0.10 eV.

At the other end of the valence-bands — the "bottom" or high

binding energy limit — it is more difficult to establish exactly

where the bands end, although XPS spectra tend to be more readily

interpretable in this respect than either SXS or UPS data. Most of

our spectra show some tailing at the "bottom" of the valence bands.

This tailing may be a real physical effect for it persists even after

subtraction of the inelastic tail through the assumption that each

point in I(E) contributes to the inelastic tail in proportion to its

initial intensity. In any case, some interpretation is necessary to

assign the positions of the bottoms of the valence bands. The bottom

of the valence bands for Sc and Fe is well defined by the negative

curvature in I(E) in this region. The spectra of Ti through Mn

exhibit a slight kink as I(E) joins the essentially flat background.

## IV. DISCUSSION

### A. Comparison With Other Experimental Results

In this section we present a short comparison of our XPS spectra

with other XPS measurements and with lower photon energy (hν ≤ 40 eV)

experiments — namely UPS and SXS.

In Fig. 3 we compare the VB spectra of Cr obtained through the

use of the UPS, SXS, and XPS methods. The soft x-ray spectrum (SXS)

was obtained by Fischer;[4] it represents the Cr (2p-hole) → Cr(VB-hole)

transitions. The UPS spectrum is from Eastman[13] at photon energy of

10.2 eV and the XPS spectrum is from this work. The three spectra

indicate a region of high electron intensity around -2.0 eV and similar

band full-width at half maximum (FWHM) of 4.9 eV (XPS), 4.6 eV (UPS),

and 4.5 eV (SXS). The energies of the fine structure in these spectra

vary considerably from one method to the other. Also, more recent

UPS spectra of Cr[33] taken with the HeI and HeII lines have different

appearances from those in Fig. 3. For Ti, the SXS spectrum taken

by Fischer and Baun[7] does not agree well with XPS and UPS data, which

agree with each other quite well in this case. Similarily for Fe,[13,21,34]

Pessa, et al.[21] had good agreement between their UPS spectrum at 16.84 eV

and the XPS spectrum

It can be concluded, therefore, that the degrees of actual corres-

pondence of UPS and XPS spectra can be interpreted as a measure of the

structure introduced into the UPS spectrum by the final states along

with the differences in cross-section modulation in the two energy

regimes.

Our present XPS results agree quite well with earlier XPS data on

Fe, in particular those of references 26 and 27. The spectrum reported

by Szalkowski and Megerle[25] is not in as good an agreement. Our Mn spec-

trum has slightly better statistics than that reported by Hüfner and

Wertheim;[27] however, the agreement between the two spectra is quite

good.

## B. Comparison With Theory

In comparing our spectra with the theoretical density of

states N(E) obtained through band structure calculations, we will

assume that the "density of ionization potentials", our measured I(E),

resembles N(E). The implications of this assumption have been discussed elsewhere[15,23,35] and will not be reported here. At the same time, we note that attempts to interpret I(E) in terms of N(E) may be regarded as a test of the applicability of this procedure.

In the following we will compare our XPS spectra separately with theoretical results for each of the metals studied.

1. Scandium and Titanium

Scandium and titanium start the 3d transition metal series with atomic configurations $3d^1 4s^2$ and $3d^2 4s^2$ respectively. They both crystallize in an hcp lattice with a c/a ratio of 1.59.

This structural identity introduces an element of rigidity into the band structure, which is borne out quite clearly in the high energy part of I(E), if we line up the shoulders of the peaks labeled B in I(E) for scandium and titanium (compare Fig. 1). Between peak B and the Fermi level $E_F$, I(E) rises to form a second peak in Ti while scandium $E_F$ intersects N(E) before the peak is reached. Finite resolution of the spectrometer moves the break in intensity to a point 0.4 eV below $E_F$. The titanium valence bands have to accommodate one more electron, and $E_F$ is accordingly shifted up 0.5 eV. Thus, the second peak A in the density of states is occupied beyond its maximum and $E_F$ intersects a region of lower density with the break in I(E) again shifted down 0.4 eV by instrumental broadening.

Toward lower energy, I(E) tails off in a similar way for both metals. The bottom of the valence bands is, in each case, tentatively assigned to a kink E which occurs at approximately $(E_F - 8.3)$ eV for

Sc and $(E_F - 8.1)$ eV for Ti.

A closer inspection reveals some important differences in detail. Between peak B and edge D, the scandium spectrum tails off in an s-like shape with an inflection point C around ~4 eV. In titanium, we can just distinguish a discontinuity in slope marked C in Fig. 1.

The density of states N(E) for scandium and titanium has been calculated by Altmann and Bradley[36,37] using the cellular method. We compare their results with our spectra in Fig. 4. The energies of characteristic features are set out in Table II.

The agreement in the overall shape of N(E) and I(E) is good for Sc and fair for Ti. Notice especially the two peaks A and B and the change in position of $E_F$ relative to peak A from scandium to titanium. The repeated changes in the curvature of I(E) between B and E in scandium as opposed to the essentially smooth decrease of I(E) in the same region in titanium agree quite well with the Altmann and Bradley calculation. The lack of resolution in their N(E) histograms, however, obviates the identification of feature C in the titanium spectrum.

This quite satisfactory overall picture is marred by considerable discrepancies in the energies of characteristic features between N(E) and I(E), the exception being the total bandwidth of titanium (compare Table II). The different directions in which the upper and lower parts of N(E) deviate from their experimental counterparts may reflect the different origins of the regions in terms of atomic orbitals. These differences make the matching of features C and D in I(E) for scandium with similar ones in N(E) rather arbitrary.

Mattheiss[38] has calculated the band structure of titanium along the Γ-K symmetry direction using the augmented plane wave method (APW). His total bandwidth of 6.3 eV falls considerably short of the 8.1 eV measured in this experiment. Hygh and Welch[39] have also done several APW calculations on Ti. Their bandwidths also fall short of experiment but their density of states does show a two-peak structure. It would be interesting to compare our results with more recent APW[40] and LCAO[41] calculations when the calculated densities become available. The APW bands calculated for Sc by Fleming and Loucks[42] are likewise considerably narrower than observed. Das, et al.[43] have recently performed an RAPW calculation on Sc. Their density of states compares qualitatively with our XPS results but again are much too narrow.

## 2. Vanadium and Chromium

Vanadaium and chromium, with 5 and 6 valence electrons, respectively, crystallize in the relatively open body-centered cubic (bcc) structure.

Chromium is an antiferromagnet at room temperature with a spin arrangement in the form of a spin-density wave. The wavelength is slightly less than twice the periodicity of the chemical lattice. Disregarding this difference, Asano and Yamashita[44] have treated the band structure of an idealized antiferromagnetic chromium by invoking the concept of a magnetic superlattice with twice the ordinary lattice constant. This reduces the Brillouin zone (BZ) of the bcc lattice and introduces gaps of the order of 0.4 eV at points where bands cross the new zone boundaries. Though the occurrence of these gaps at the

Fermi energy is essential for the stabilization of the antiferromagnetic order[45] in Cr, we do not expect them to alter the overall density of states strongly because they occur at different energies for different bands. This explains the great similarity in the densities of states derived by Connolly[46] for the band-structure calculations of paramagnetic and antiferromagnetic Cr by Asano and Yamashita.[44] It is therefore reasonable to compare our measurements with calculations on the paramagnetic state of bcc chromium.

Densities of states $N(E)$ have been calculated by several authors. The best agreement between theory and experiment is found in the APW calculations by Gupta and Sinha,[47] shown in Fig. 5. The overall agreement between $N(E)$ and our experimental spectrum is quite good. The edge at 4.9 eV in $N(E)$ marks the position of the symmetry points $H_{12}$ and $N_1$ and thus the bottom of the d bands. The spike in $N(E)$ at 2.4 eV arises from the flat bands connecting $P_4$ and $N_2$ along the PN edge of the bcc Brillouin zone (BZ). The high spike at 1.4 eV on $N(E)$ is not readily attributable to any particular region in the BZ. In agreement with the band structure calculation we find that $I(E)$ is quite low near $E_F$. This feature has not been previously observed by the UPS or SXS methods.

A tail due mainly to a 4s-derived band extends down to 8.5 eV in $N(E)$. This agrees reasonably well with the value $8.8 \pm 0.3$ eV determined for the total valence bandwidth of chromium from our spectrum. The d-band densities of states calculated by Asdente and Friedel[48] using a tight-binding scheme agrees in general shape with our spectrum, as does the APW calculation of Snow and Waber.[49] Energies of symmetry

points from four recent calculations[47,50,51] are compared with values

deduced from our spectrum in Table III. It is clear from this that

the agreement between the different theories and our spectrum is

rather good, though the tight-binding calculations[50,51] give narrower

bands.

The valence-band spectrum of vanadium is very similar to that of

chromium. Allowing for a shift in the Fermi level $E_F$ due to the reduc-

tion by one in the number of valence electrons, we find a one-to-one

correspondence in the characteristic features of the two spectra. In

vanadium, $E_F$ has moved down toward the higher peak by about 1 eV. The

separation between the two main peaks is almost the same of about 1.8 eV.

In vanadium, both peaks appear narrower. This reduction in d-band

dispersion is presumably due to the slightly increased atomic spacing

of vanadium as compared to chromium. In Fig. 5 we compare the Cr

density of states of Gupta and Sinha,[47] shifted toward $E_F$ by 1 eV,

with our vanadium spectrum. Peak A marks the maximum near symmetry

points $P_4$ and $N_2$. The energies of $H_{12}$ and $N_1$ at the bottom of the

d bands are well-defined in the vanadium spectrum at $(3.5 \pm 0.3)$ eV

below $E_F$. The detailed picture that we have obtained for the density

of the states of Cr and V will aid us in interpretation of the Fe

spectrum.

3. Manganese

Manganese crystallizes in a distorted cubic lattice with 29 atoms

per primitive cell. No band structure has therefore as yet been cal-

culated. The VB-spectrum (see Fig. 2) shows a broad bump with a total

width of $8.8 \pm 0.3$ eV. A peak A at $(E_F-1.1)$ eV and a shoulder B at

$(E_F-4.1)$ eV can be distinguished in $I(E)$. Judging from the steep

slope at $E_F$, the density at $E_F$ is probably close to its maximum value.

## 4. Iron

The band model of ferromagnetism due to Stoner, Wohlfarth, and

Slater (SWS)[52-53] features spin-polarized bands $\varepsilon_n(\vec{k})$ which are split

by energies $\Delta E_n(\vec{k})$ due to the exchange interaction. $\Delta E$ is a function

of wavevector $\vec{k}$ and band index $n$ but it has usually been treated as

a constant for d-derived bands and is set equal to zero for sp-derived

bands. Estimates[54] for the average exchange splitting of the d bands

$\Delta E$ are about 0.4 eV in Ni, 1.1 eV in Co, and 1.7 eV in Fe.

More recently, band structure calculations of ferromagnetic Fe

by Tawil and Callaway[55] have derived the exchange splitting $E_n(\vec{k})$ self-

consistently using an average Hartree-Fock field that is different for

the two electron spin directions. These calculations reproduce the

observed saturation moments quite satisfactorily.

Schemes different from the SWS-model have been proposed[56] which

emphasize intra-atomic exchange and correlation effects in the forma-

tion of spin-ordered structures. However, to our knowledge, no explicit

calculations have been made which would bear direcly on the electronic

structure of ferromagnetic transition metals.

Two of the implications of the SWS model have been tested exten-

sively:

(1) The spin polarization of electrons at the Fermi energy $E_F$

is well established[57,58] and can be explained both in sign and magnitude

by the SWS model.[59]

(2) A number of spectroscopic techniques have been employed to study the changes in the band structure which are supposed to accompany the transition from the ferromagnetic to the paramagnetic state as $\Delta E$ goes to zero at the Curie temperature $T_c$.[5,8,34,60,61] The effects observed are however very small and do not readily lend themselves to a straightforward interpretation in terms of the SWS model.

In this inconclusive situation let us rephrase the question put forward by previous investigators from: "Does the band structure of a metal change according to the SWS-model if we cross the Curie temperature $T_c$?" to "Does the SWS-model give an appropriate description of the density of states $N(E)$ of a ferromagnetic transition metal like iron below $T_c$?".

To answer this question, let us first consider the $N(E)$ curve for chromium (Fig. 5) which we have found to be in good agreement with our XPS spectrum. Because iron and chromium crystallize in the same bcc structure and have only slightly different lattice constants, we may regard this curve as a fair representation of $N(E)$ for iron in the unmagnetized state. The Fermi energy $E_F$ for this state would fall right at the top of the high density peak, as shown in Fig. 6a. The chemical potentials for spin up ($\lambda_\uparrow$) and spin down ($\lambda_\downarrow$) can easily be determined by allowing for the appropriate magnetic moment in ferromagnetic iron and assuming a rigid-band exchange splitting $\Delta E$. In the final step, $\lambda_\uparrow$ and $\lambda_\downarrow$ coincide to form the new Fermi level in the SWS description of the ferromagnetic state. It is clear from Fig. 6b.

that this new density of states differs drastically from the non-polarized N(E). Instead of a peak, we now have a region of low electron density at $E_F$ and a peak about 1.8 eV below $E_F$.

These two features are common to all N(E) calculations for Fe employing the SWS model and we find just these features in our XPS spectrum of iron, shown in Fig. 7 together with N(E) derived by Connolly[46] from the energy bands of Wakoh and Yamashita.[62]

As can be seen from Fig. 7 the agreement is quite good and details are well reproduced. The bottom of the d bands is marked in the calculations, by and edge in N(E) between 4.5 and 5.0 eV. Structure C in I(E), by Connolly and by Tawil and Callaway which presumably corresponds to this point lies at least 0.5 eV lower. The bottom of the valence bands is marked at 9.2 eV by the intercept of the parabolic sp band with the baseline. The calculated values for the same point $\Gamma_1$ again fall short of this value by about 1.4 eV.

A very detailed treatment of the exchange problem in the band structure of ferromagnetic iron has been given by Duff and Das.[63] As a result they obtained significantly greater exchange splittings throughout the Brillouin zone as compared to other calculations. This increased the overall bandwidth to 13 ev and the d-bandwidth (point C in I(E)) to 9.9 eV, both of which exceed the experimental values considerably. It is, however, clear from their calculation how assumptions about screening and the localizing effect of correlation influence the exchange and therefore the bandwidths. With the data provided by our spectra we hope that information about the real magnitude of these many-body effects for the ferromagnetic state may be obtained.

Let us return to the question of whether the SWS-model is appropriate for describing N(E) for ferromagnetic metals. The answer we believe is "yes" from all we have seen in the interpretation of our XPS data here and in Ni and Co.[24] But why do the above mentioned experiments fail to detect the collapse of the exchange splitting above the Curie temperature? To qualify this question we have to consider two things: what has been measured and what does "above $T_c$" mean. Above $T_c$ means in all these cases not more than 1.07 $T_c$. And the quantity measured was closely related to the density of states, which is well known to be already quite well developed for clusters of only 10 to 20 atoms.[64]

The negative results of these experiments then mean that at 1.07 $T_c$ there is still a nonvanishing spin density over a region covering a cluster of atoms. This is quite compatible with the loss of any long-range spin order and with the nature of the magnetic transition as a second-order transition.

-17-

## ACKNOWLEDGEMENTS

-18-

REFERENCES

1. L. Hodges, R. E. Watson, and H. Ehrenreich, Phys. Rev. B5, 3953 (1972).

2. For a review see C. Herring, Magnetism, ed. by G. T. Rado and H. Suhl (Academic Press, New York, 1966), Vol. IV.

3. D. W. Fischer, J. Appl. Phys. 40, 4151 (1969).

4. D. W. Fischer, Phys. Rev. B4, 1778 (1971).

5. R. C. Dobbyn, M. L. Williams, J. R. Cuthill, and A. J. McAlister, Phys. Rev. B2, 1563 (1970).

6. A. J. McAlister, J. R. Cuthill, R. C. Dobbyn, M. L. Williams, and R. E. Watson, Phys. Rev. Lett. 29, 179 (1972); Phys. Rev. B12, 2973 (1975).

7. D. W. Fischer and W. L. Baun, J. Appl. Phys. 39, 4757 (1968).

8. D. T. Pierce and W. E. Spicer, Phys. Rev. Lett. 25, 581 (1970).

9. C. N. Berglund and W. E. Spicer, Phys. Rev. 136, A1030 (1964); ibid. 136, A1044 (1964).

10. A. J. Blodgett, Jr. and W. E. Spicer, Phys. Rev. 146, 390 (1966).

11. A. Y.-C. Yu and W. E. Spicer, Phys. Rev. Lett. 23, 1171 (1966).

12. A. J. Blodgett and W. E. Spicer, Phys. Rev. 158, 514 (1967).

13. D. E. Eastman, J. Appl. Phys. 40, 1387 (1969).

14. D. E. Eastman, Sol. St. Comm. 7, 1697 (1969); D. E. Eastman, Electron Spectroscopy, ed. by D. A. Shirley (North-Holland Publishing Co., Amsterdam, 1972); p. 487.

15. C. S. Fadley and D. A. Shirley, Electronic Density of States, Bur. Std. (U.S.A.) Special Publication 323, 163 (1971).

16. G. D. Mahan, Phys. Rev. 163, 612 (1967); C. Kunz, R. Haensel, G. Keitel, P. Schreiber, and B. Sonntag, Electronic Density of States, Nat. Bur. Std. (U.S.A) Special Publication 323, 253 (1971).

17. See for example, W. E. Spicer in Electronic Density of States, Nat. Bur Std. Special Publication 323, 139, 191 (1971).

18. See for example, W. F. Krolikowski and W. E. Spicer, Phys. Rev. 185, 882 (1969).

19. a) N. V. Smith, Electronic Density of States, Nat. Bur. Std. Special Publication 323, 191 (1971).

    b) M. M. Traum and N. V. Smith, Phys. Rev. B9, 1353 (1974).

20. A. R. Williams, J. F. Janak, and   Moruzzi, Phys. Rev. Lett. 28, 671 (1972).

21. M. Pessa, P. Heimann, and H. Neddermeyer, Phys. Rev. B14, 3488 (1976).

22. D. E. Eastman and W. D. Grobman, Phys. Rev. Lett. 28, 1327 (1972).

23. L. Ley, R. A. Pollak, F. R. McFeely, S. P. Kowalczyk, and D. A. Shirley, Phys. Rev. B9, 600 (1974).

24. L. Ley, S. P. Kowalczyk, F. R. McFeely, and D. A. Shirley, Lawrence Berkeley Laboratory Report 2929, 1974 (unpublished).

25. F. J. Szalkowski and C. A. Megerle, Phys. Lett. 48A, 117 (1974).

26. H. Höchst, A. Goldman, and S. Hüfner, Z. Phyzik B24, 245 (1976).

27. S. Hüfner and G. K. Wertheim, Phys. Lett. 47A, 349 (1974).

28. Y. Baer, P. F. Hedén, J. Hedman, M. Klasson, C. Nordling, and
    K. Siegbahn, Physica Scripta 1, 55 (1970).

29. R. A. Pollak, S. P. Kowalczyk, L. Ley, and D. A. Shirley, Phys.
    Rev. Lett. 29, 274 (1972).

30. T. E. Madey, J. T. Yates, and N. E. Erickson, Chem. Phys. Lett.
    19, 487 (1973).

31. D. R. Penn, J. Elect. Spect. and Rel. Phen. 19, 29 (1976).

32. R. C. G. Leckey, Phys. Rev. A13, 1043 (1976).

33. P. J. Page and P. M. Williams, Vacuum Ultraviolet Radiation
    Physics, eds. E. Koch, R. Haensel, and C. Kunz (Pergamon-Vieweg,
    1974), p. 566.

34. L.-G. Petersson, R. Melander, D. P. Spears, and S. B. M. Hagström,
    Phys. Rev. B14, 4177 (1976).

35. L. Ley, S. P. Kowalczyk, F. R. McFeely, R. A. Pollak, and D. A.
    Shirley, Phys. Rev. B8, 2392 (1973).

36. S. L. Altmann and C. J. Bradley, Proc. Phys. Soc. (London) 92,
    764 (1967).

37. S. L. Altmann and C. J. Bradley, Soft X-ray Band Spectra, ed.
    D.J. Fabian (Academic Press, New York, 1968), p. 265.

38. L. F. Mattheiss, Phys. Rev. 134, A970 (1964).

39. E. H. Hygh and R. M. Welch, Phys. Rev. B1, 2424 (1970); R. M.
    Welch and E. H. Hygh, Phys. Rev. B4, 4261 (1971); R. M. Welch
    and E. H. Hygh, Phys. Rev. B9, 1993 (1974).

40. R. A. Tawil and J. Rath, private communication (1977).

-21-

41. R. A. Tawil and T. J. Green, Arab. J. Sci. Engin. $\underline{2}$ (to appear in 1977).

42. G. S. Fleming and T. L. Loucks, Phys. Rev. $\underline{173}$, 685 (1968).

43. S. G. Das, A. J. Freeman, D. D. Koelling, and F. M. Mueller, Magnetism and Magnetic Materials-1972, eds. C. D. Graham, Jr. and J. J. Rhyne (American Institute of Physics, New York, 1973), p. 1304.

44. S. Asano and J. Yamashita, J. Phys. Soc. (Japan) $\underline{23}$, 714 (1967).

45. W. M. Lomer, in Proc. Int. School of Physics, E. Fermi, Course XXXVII, ed. W. Marshall (Academic Press, New York, 1967).

46. J. W. D. Connolly, Electronic Density of States, Nat. Bur. Std. Special Publication $\underline{323}$, 27 (1971).

47. R. P. Gupta and S. K. Sinha, Phys. Rev. $\underline{B3}$, 2401 (1971).

48. M. Asdente and J. Friedel, Phys. Rev. $\underline{124}$, 384 (1961).

49. E. C. Snow and J. T. Waber, Acta Metall. $\underline{17}$, 623 (1969).

50. M. Yasin, E. Hayashi, and M. Shimiga, J. Phys. Soc. Japan $\underline{29}$, 1440 (1970).

51. J. Rath and J. Callaway, Phys. Rev. $\underline{B8}$, 5398 (1973).

52. E. C. Stoner, Phil. Mag. $\underline{15}$, 1018 (1933); E. P. Wohlfarth, Rev. Mod. Phys. $\underline{25}$, 211 (1953).

53. J. C. Slater, Phys. Rev. $\underline{49}$, 537, 931 (1936).

54. E. P. Wohlfarth, Proc. Int. Conf. Magnetism (Institue of Physics and Physical Society of London, Nottingham, England, 1965), p. 51.

55. R. A. Tawil and J. Callaway, Phys. Rev. $\underline{B7}$, 1242 (1973); also, C. S. Wang and J. Callaway (to be published).

56. See for example, J. H. Van Vleck, Rev. Mod. Phys. $\underline{25}$, 220 (1953).

57. U. Banninger, G. Bush, M. Campagna, and H. C. Siegmann, Phys. Rev. Lett. 25, 585 (1970).

58. W. Gluich, G. Regenfus, and R. Siegmann, Phys. Rev. Lett. 27, 1066 (1971).

59. B. A. Politzer and P. H. Cutler, Phys. Rev. Lett. 28, 1330 (1972).

60. C. S. Fadley and D. A. Shirley, Phys. Rev. Lett. 21, 980 (1968).

61. J. E. Rowe and J. C. Tracy, Phys. Rev. Lett. 27, 799 (1971).

62. S. Wakoh and J. Yamashita, J. Phys. Soc. Japan 21, 1712 (1966).

63. K. J. Duff and T. P. Das, Phys. Rev. B3, 192 (1971).

64. P. J. Jennings, G. S. Painter, and R. O. Jones, Surface Science 60, 255 (1976).

Table I.  Energies of characteristic features in the valence band spectra of the transition metals.  Errors are given parenthetically.  Entires are in eV.

| Element | A | B | C | D | E |
|---------|--------|--------|--------|--------|--------|
| Sc | 0.4(1) | 1.4(2) | 3.6(3) | 5.6(3) | 8.3(4) |
| Ti | 0.7(1) | 1.7(2) | 4.2(2) | — | 8.1(3) |
| V | 0.6(1) | 2.4(2) | 5.0(3) | — | 9.1(3) |
| Cr | 1.8(1) | 2.6(2) | 3.5(3) | — | 8.8(3) |
| Mn | 1.1(1) | 4.1(3) | — | — | 8.7(4) |
| Fe | 0.8(1) | 1.9(2) | 4.9(5) | — | 9.2(4) |

Table II. A comparison of structural features in the valence band spectrum of scandium and titanium with the corresponding densities of states calculated by Altmann and Bradley.[34,35] The entries are in eV below the Fermi energy $E_F$. Errors are given parenthetically.

| | Sc | | Ti | |
|---|---|---|---|---|
| | Expt. | Theory | Expt. | Theory |
| $E_F$ | 0 | 0 | 0 | 0 |
| peak A | 0.4(1) | 0.0 | 0.7(1) | 1.0 |
| peak B | 1.4(2) | 1.7 | 1.7(2) | 3.4 |
| inflection point C | 3.6(3) | 2.4 | 4.2(2) | —— |
| inflection point D | 5.6(3) | 3.6[a] | —— | —— |
| bottom of VB E | 8.3(4) | 6.0 | 8.1(3) | 8.0 |

[a] The identification of features C and D in N(E) is ambiguous (see text).

Table III. Energies of symmetry points in the valence bands of chromium (eV below $E_F$).

| Symmetry Point | Tight-binding plus OPW[a] | | Tight-binding, SCF[b] $\alpha = 2/3$ | APW, $\alpha = 1$[c] | Expt., this work |
|---|---|---|---|---|---|
| | $\alpha = 1$ | $\alpha = 0.725$ | | | |
| $\Gamma'_{25}$ | 1.0 | 1.0 | 1.0 | 0.7 | |
| $P_4$ | 1.6 | 2.0 | 2.2 | 2.5 | 2.6(2) |
| $N_2$ | 2.3 | 2.4 | 2.7 | 2.4 | |
| $H_{12}$ | 3.0 | 3.3 | 4.0 | 4.8 | 3.5(3) |
| $N_1$ | 3.3 | 3.9 | 4.3 | 4.9 | |
| $\Gamma_1$ | 5.1 | 6.9 | 5.9 | 8.7 | 8.8(3) |

[a] Ref. 50. Here $\alpha$ is the exchange parameter.
[b] Ref. 51.
[c] Ref. 47.

FIGURE CAPTIONS

Fig. 1.  X-ray photoemission spectrum I(E) of the valence band region

of Sc, Ti, and V.  The sum of the counts in four adjacent

channels is represented by points joined with straight lines.

The points are approximately 0.16 eV apart.  The features,

denoted by letters, are discussed in the text and the energies

are given in Table I.

Fig. 2.  X-ray photoemission spectrum I(E) of the valence band region

of Cr, Mn, and Fe.  The sum of the counts in four adjacent

channels is represented by points joined with straight lines.

The points are approximately 0.16 eV apart.  The features,

denoted by letters, are discussed in the text and the energies

are given in Table I.

Fig. 3.  A comparison of the valence band spectra of Cr obtained by

ultraviolet photoemission (UPS, Ref. 13), soft x-ray spec-

troscopy (SXS, Ref. 4) and x-ray photoemission (XPS, this

work).

Fig. 4.  A comparison of the x-ray photoemission valence band spectra

I(E) (upper curves) with density of states N(E) (lower curves)

calculated by Altmann and Bradley (Refs. 36 and 37) for Sc

and Ti.  The energies of the characteristic features are

given in Table II.

Fig. 5.   The x-ray photoemission valence band spectra I(E) of V and

Cr are compared with the APW results of Gupta and Sinha

(Ref. 47).  For V we have used Gupta and Sinha's Cr density

of states with the Fermi level shifted corresponding to the

reduction by one of the number of valence electrons by one

electron.

Fig. 6.   a) The bcc chromium density of states (Ref. 47) $\lambda_\downarrow$ and $\lambda_\uparrow$,

the spin up and spin down chemical potentials for bcc Fe are

determined from the magnetic moment of Fe under the assump-

tion of a rigid band exchange splitting.

b) The resulting spin-polarized density of states where

the chemical potentials $\lambda_\downarrow$ and $\lambda_\uparrow$ have been made to coincide.

This density of states should be representative for that

of ferromagnetic iron.

Fig. 7.   A comparison of the x-ray photoemission valence band spectrum

I(E) of Fe (upper curve) with the N(E) derived by Connolloy

(Ref. 46) (lower curve).
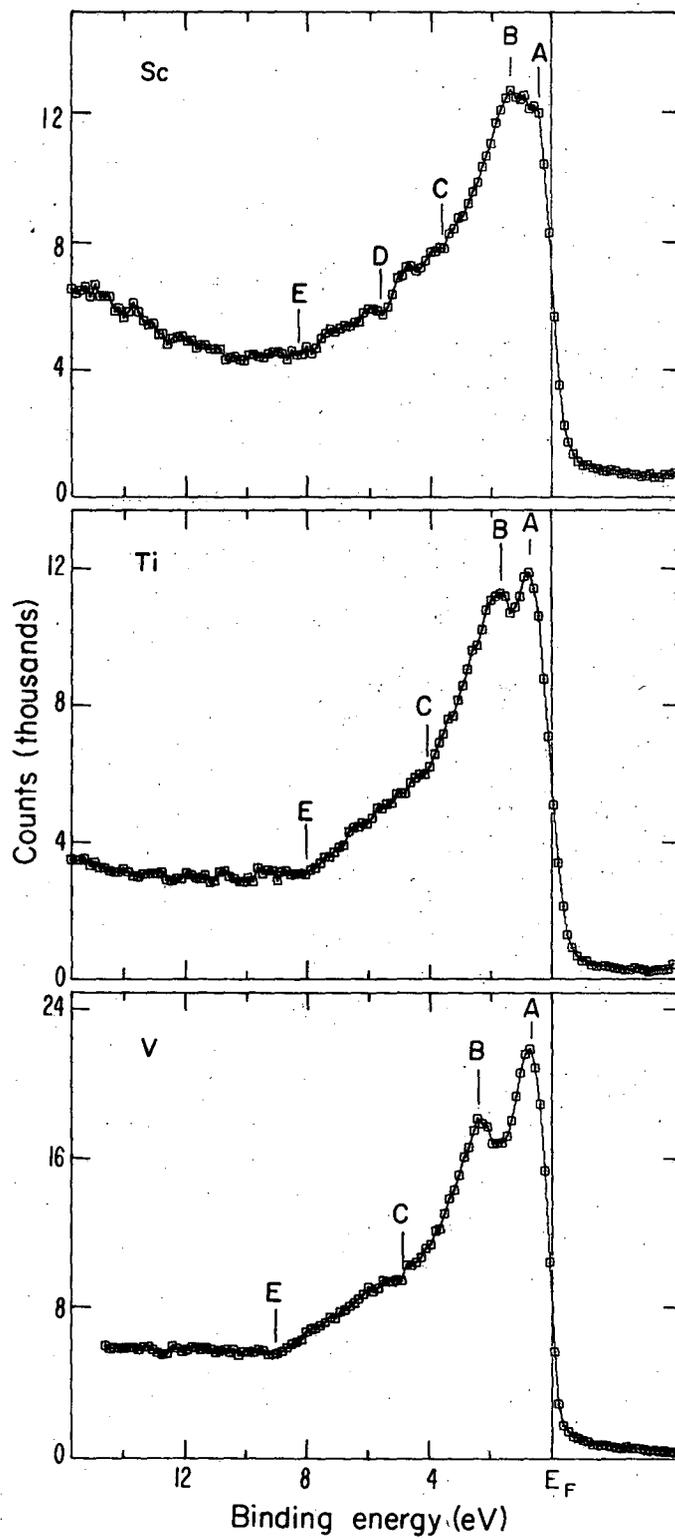
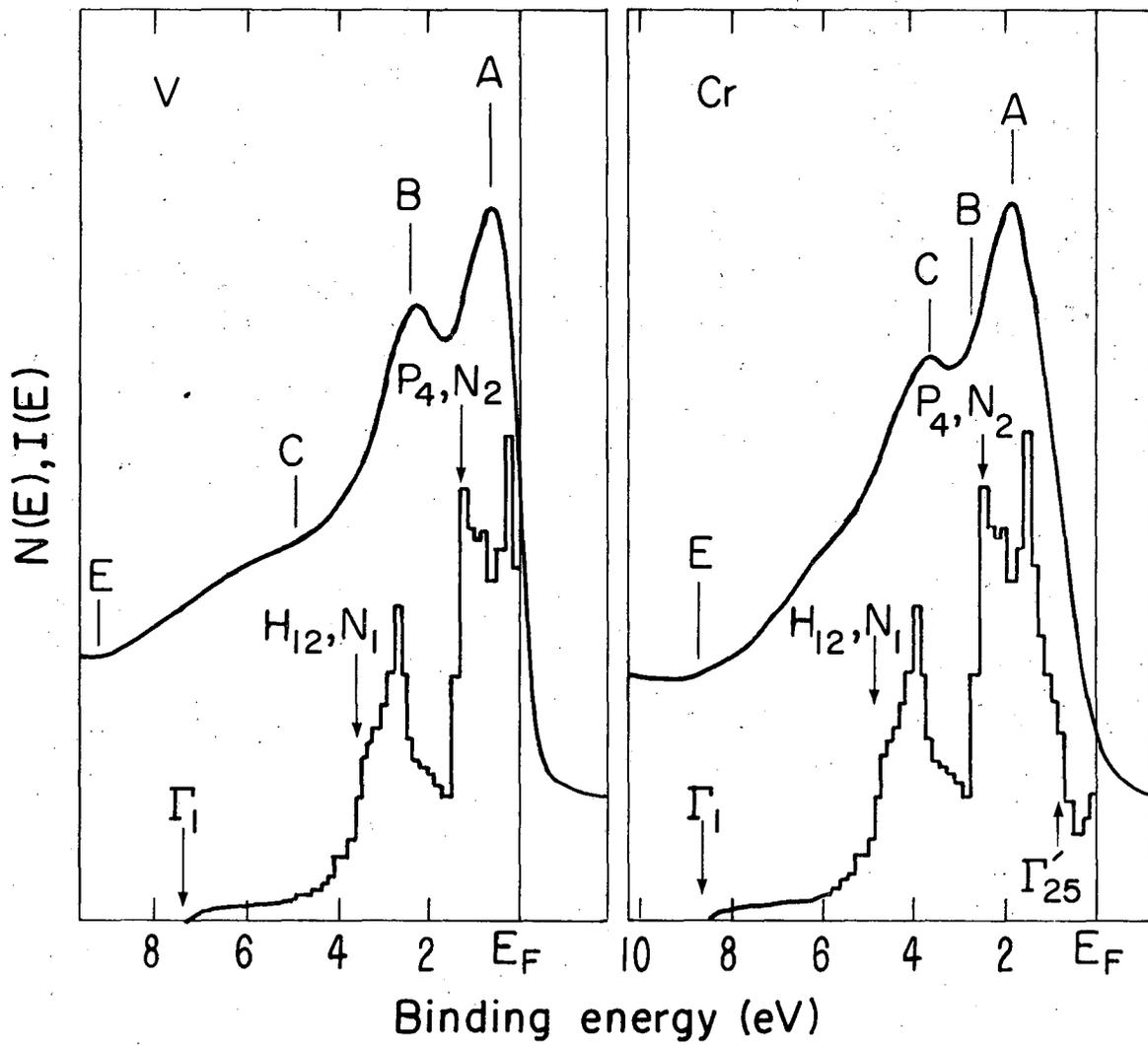Fig. 1    XBL 774-879
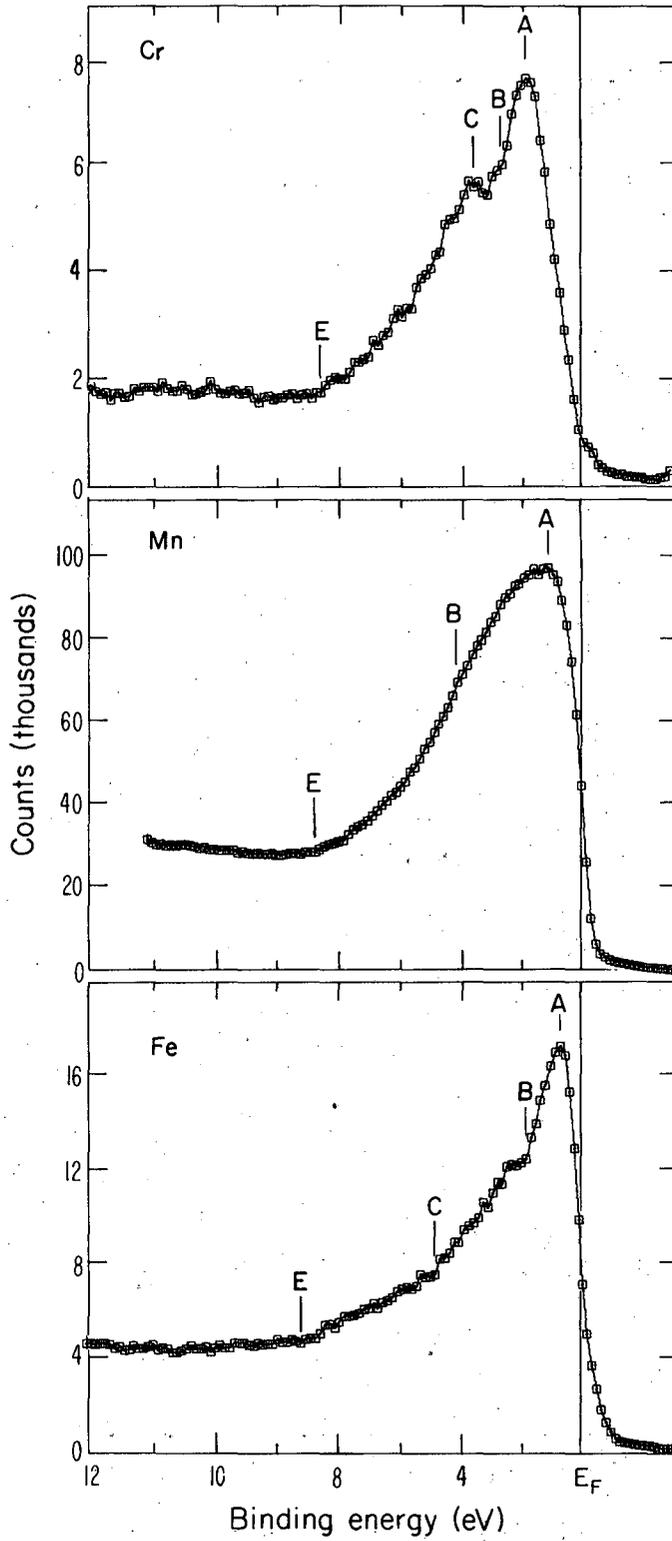
Fig. 2

XBL 774-878

Fig. 3

XBL 774-877

Fig. 4

XBL 774-874

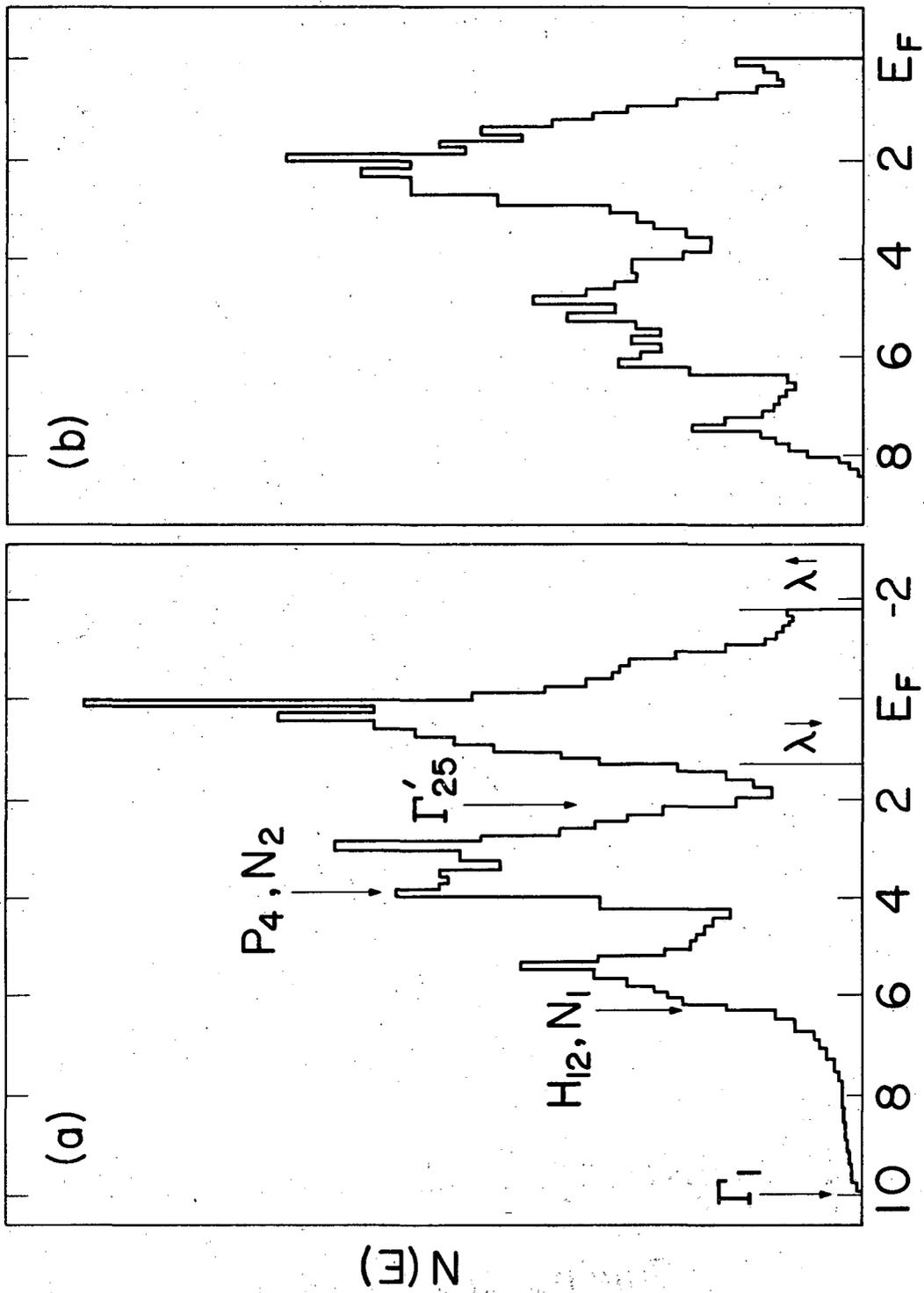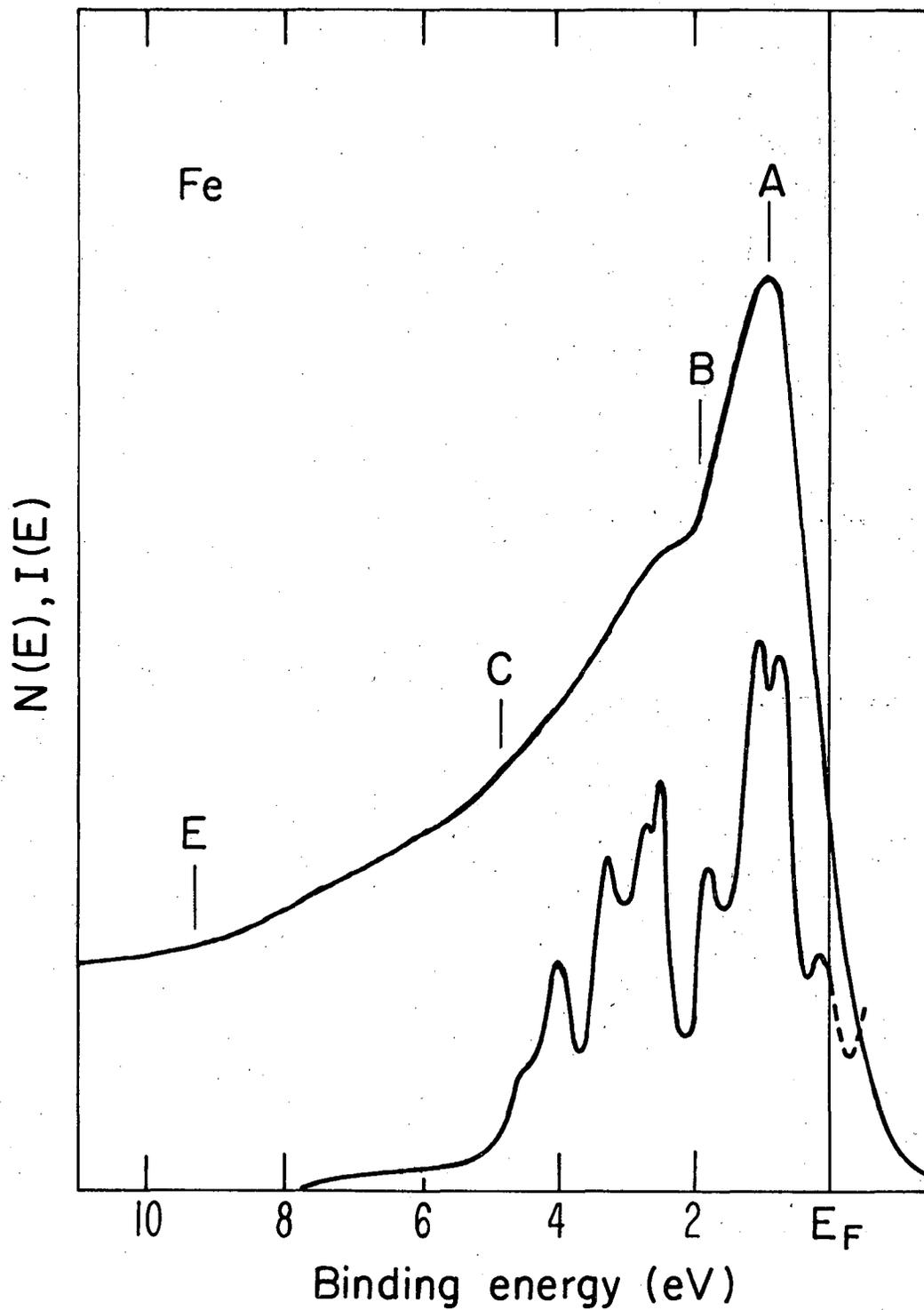Fig. 5

XBL 774-875

Fig. 6

XBL 747-3644

Fig. 7

0 0 0 0 4 7 1 0 4 9 6